

# Parameter identification of PMSM based on dung beetle optimization algorithm

XIAOLIANG YANG<sup>1,2</sup>  , YUYUE CUI<sup>1,2</sup>, LIANHUA JIA<sup>3</sup>, ZHIHONG SUN<sup>3</sup>,  
PENG ZHANG<sup>3</sup>, JIANE ZHAO<sup>4</sup>, RUI WANG<sup>1,2</sup>

<sup>1</sup>*School of Electrical and Information Engineer, Zhengzhou University of Light Industry  
Zhengzhou, China*

<sup>2</sup>*Henan Key Lab of Information based Electrical Appliances  
Zhengzhou, China*

<sup>3</sup>*China Railway Engineering Equipment Group Co. Ltd  
Zhengzhou, China*

<sup>4</sup>*School of Electrical and Electronic Engineering, Zhengzhou University of Science and Technology  
Zhengzhou, China*

*e-mail: [yangxl@hnu.edu.cn](mailto:yangxl@hnu.edu.cn)*

(Received: 05.05.2023, revised: 07.09.2023)

**Abstract:** In this paper, a creative dung beetle optimization (CDBO) algorithm is proposed and applied to the offline parameter identification of permanent magnet synchronous motors. First, in order to uniformly initialize the population state and increase the population diversity, a strategy to improve the initialization of the dung beetle population using Singer chaotic mapping is proposed to improve the global search performance; second, in order to improve the local search performance and enhance the convergence accuracy of the algorithm, a new dung beetle position update strategy is designed to increase the spatial search range of the algorithm. Simulation results show that the proposed optimization algorithm can quickly and accurately identify parameters such as resistance, inductance, and magnetic chain of the PMSM, with significant improvements in convergence algebra, identification accuracy and stability.

**Key words:** chaotic mapping, dung beetle algorithm, Levy flight, parameter identification, permanent magnet synchronous motor, spiral strategy

## 1. Introduction

In recent years, permanent magnet synchronous motors (PMSMs) have been widely used in industry, household appliances and electric vehicles because of their simple design, low rotational inertia, high acceleration, high torque, high overload capacity, high power-to-weight ratio, and



© 2023. The Author(s). This is an open-access article distributed under the terms of the Creative Commons Attribution-NonCommercial-NoDerivatives License (CC BY-NC-ND 4.0, <https://creativecommons.org/licenses/by-nc-nd/4.0/>), which permits use, distribution, and reproduction in any medium, provided that the Article is properly cited, the use is non-commercial, and no modifications or adaptations are made.

wide speed regulation range and high efficiency [1]. In widely used speed sensorless systems, the accuracy of magnetic field orientation depends on the accuracy of motor parameters. In order to effectively improve the control performance of motors, it is necessary to obtain accurate parameter information of motors, therefore, the PMSM offline parameter identification method has become the main object of research by domestic and foreign scholars [2].

Commonly used traditional methods are Recursive Least Squares (RLS) [3], Multivariate Adaptive Regression Splines (MARS) [4], Extended Kalman Filter (EKF) [5,6] method, etc. The RLS method for motor parameter identification, the principle of this method is simple and easy to implement, but the phenomenon of data saturation will occur, which is not conducive to practical applications. MARS for motor parameter identification, this method is less difficult to implement, but requires the derivation of the corresponding adaptation laws, taking into account the influence of coupling and the accuracy of its parameters, otherwise non-convergence and errors can occur. Based on the EKF algorithm for parameter identification, although the algorithm is suitable for high-performance servo systems, the results are influenced by the initial value, which not only makes the robustness of parameter identification reduced but also affects the identification accuracy.

In recent years, intelligent optimization algorithms have blossomed, and they have not only made achievements in artificial intelligence, but also been widely used in the field of motor control, mainly in parameter identification, fault judgment, model prediction and so on. Due to the non-linear time-varying characteristics of PMSM control systems, it is quite difficult to identify the exact motor parameters, and convergence performance, computational power, cost and other factors need to be taken into account, using the above traditional methods often cannot quickly find the optimal value of the system [7]. Therefore, many scholars have applied intelligent optimisation algorithms to the field of parameter identification, mainly including: Particle Swarm Optimization (PSO), Sparrow Search Algorithm (SSA), Genetic Algorithm (GA), and so on. Reference [8] designed a recognition algorithm based on the standard particle swarm optimisation algorithm by introducing decreasing weights with time line type, which improves the recognition speed and accuracy to a certain extent, but the stability is poor. In Reference [9], an improved particle swarm algorithm combining the average best position and the Cauchy mutation was proposed for the first time. The algorithm has a strong search capability, high search accuracy, good stability and can be implemented under variable load conditions. Reference [10] proposes a sparrow search algorithm that combines the cross-variance strategy in the differential evolution algorithm and the incorporation of dynamic search. The algorithm can avoid falling into local optima and improve the accuracy, but the number of iterations is slightly larger. In Reference [11], a permanent magnet synchronous motor identification based on variable-step Adaline neural network is proposed, and the proposed method can effectively reduce the steady-state error of the identification results, but the convergence speed is slightly slow. In [12], an offline parameter identification method based on bat-inspired algorithm is proposed, which has the feature of good stability, but both the number of iterations and the identification error are slightly higher.

Reference [13] proposed a method to improve the initialized population of the sparrow search algorithm using Singer chaotic mapping, which increased the diversity of the initialized sparrow population and effectively improved the global search ability. References [14, 15] proposed an improved whale algorithm using the spiral strategy for location update, and after international test function analysis, the warp and algorithm improved by spiral strategy has the features of increas-

ing local search ability, preventing local prematureness and improving convergence accuracy. Reference [16] proposed a QPSO-SVM algorithm based on fusing the Levy flight strategy with adaptive variance factor optimization. For the problem of premature convergence of the QPSO algorithm, the Levy flight strategy with adaptive factors is used to correct it, which effectively improves the classification performance and prediction accuracy of the SVM. References [17, 18] propose optimization algorithms based on the Levy flight strategy, which further enables the algorithm to jump out in time when it falls into a local optimum and improves the algorithm performance. As verified by the test function [19], the algorithm is optimized and shows significant improvement in convergence accuracy, convergence speed and stability.

For the PMSM multi-parameter identification problem, a new creative dung beetle optimization (CDBO) algorithm is proposed in this paper. Firstly, a strategy to improve the initialization of dung beetle populations using Singer chaos mapping is proposed, followed by the design of a new dung beetle breeding and small dung beetle foraging location update strategy, and finally, a stolen dung beetle location update strategy. Singer chaos mapping can uniformly initialize the population state and increase the population diversity; the proposed new dung beetle breeding and small dung beetle foraging. The location update strategy makes both dung beetle breeding and small dung beetle foraging search in space in a spiral form, extending the discoverer's ability to explore unknown regions and improving the local search capability of the algorithm; the proposed stolen dung beetle location update strategy performs location update in a new way, avoiding the algorithm to limit into local optimum. The improved CDBO algorithm effectively improves the iteration speed and stability while ensuring accuracy.

This paper is divided into six parts, the second part introduces the PMSM model, the third part introduces the basic DBO algorithm, and the fourth part introduces the improved CDBO algorithm, the fifth part is the conclusion analysis, and the sixth part is the summary.

## 2. PMSM mathematical model

As a multivariable strongly coupled nonlinear system, for the purpose of analysis, the permanent magnet synchronous motor is considered as an ideal motor, ignoring core saturation, considering the spatial magnetic field as sinusoidally distributed, and disregarding factors such as core hysteresis loss and eddy current loss, using the control method of  $i_d = 0$ , the PMSM is modeled with the stator current equation in the synchronous rotating coordinate system (coordinate system) as:

$$\begin{cases} i_d = \frac{u_d + \omega_e L_q i_q}{R_s + L_d s} \\ i_q = \frac{u_q + \omega_e L_d i_d - \omega_e \psi_f}{R_s + L_q s} \end{cases}, \quad (1)$$

where:  $u_d, u_q, i_d, i_q, L_d, L_q$  are the axial voltage, current and inductance, respectively;  $R_s$  is the stator resistance;  $\psi_f$  is the permanent magnet chain; and  $\omega_e$  is the rotor electrical angular velocity.

For a model with unknown parameters, the parameter identification problem can be treated as an optimization problem. The basic idea is to identify the system parameters by continuously correcting the adjustable model through the fitness function based on the difference between the

actual output of the system and the output of the adjustable model. Generally, the dynamic model of a system can be expressed as:

$$\begin{cases} \hat{x} = f(\hat{p}, \hat{x}, u) \\ \hat{y} = g(\hat{p}, \hat{x}) \end{cases}, \quad (2)$$

where  $\hat{p}$  is the parameter vector.

To identify  $\hat{p}$ , it is necessary to compare the output of the reference model with the output of the adjustable model and measure the result of the comparison with the fitness function until the error is 0. The object function can be defined as a weighted quadratic function:

$$C(\hat{p}) = \int (y - \hat{y}) W (y - \hat{y}) dt, \quad (3)$$

where  $W$  is a positive definite matrix.

At this point, the fitness function can adjust the parameters to be identified  $\hat{p}$ , so that the identification error tends to 0 as much as possible, and the parameter identification problem is transformed into an optimization problem.

Then the motor adjustable model can be defined as:

$$\begin{cases} p\hat{i}_d = -\frac{\hat{R}_s}{\hat{L}_d}\hat{i}_d + \frac{\omega_e \hat{L}_q \hat{i}_q}{\hat{L}_d} + \frac{u_d}{\hat{L}_d} \\ p\hat{i}_q = -\frac{\hat{R}_s}{\hat{L}_q}\hat{i}_q + \frac{\omega_e \hat{L}_d \hat{i}_d}{\hat{L}_q} + \frac{u_q - \omega_e \hat{\psi}_f}{\hat{L}_q} \end{cases}. \quad (4)$$

The multi-parameter identification model of the PMSM based on the CDBO algorithm is shown in Fig. 1. In the figure,  $u_d$  and  $u_q$  represent the stator direct and cross-axis voltage;  $\omega_e$  is the rotor electrical angular velocity. The output  $i_d$  and  $i_q$  of the reference model is obtained by sampling the current sensor and then transforming it by coordinates. The output  $\hat{i}_d$  and  $\hat{i}_q$

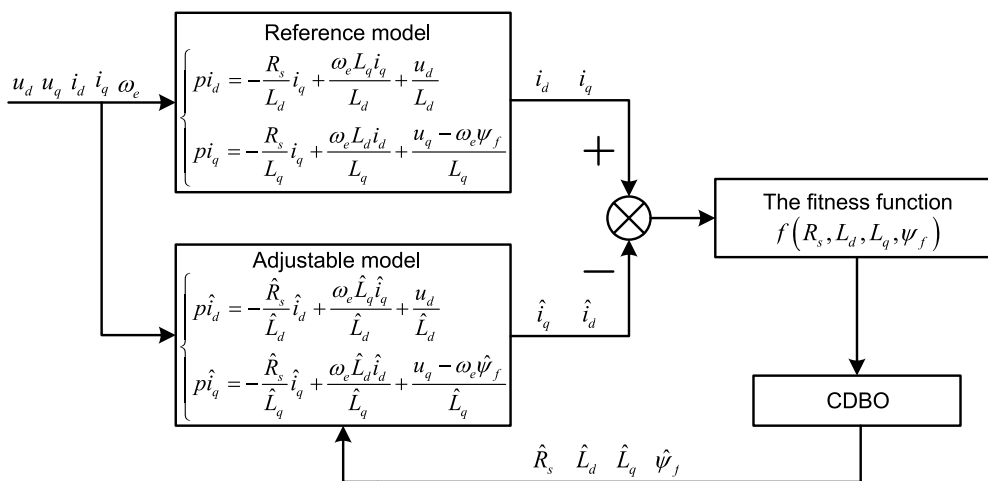


Fig. 1. PMSM parameter identification schematic

of the adjustable model is calculated by Eq. (1). The fitness of the four parameters  $R_s$ ,  $L_d$ ,  $L_q$  and  $\psi_f$ , is then obtained by the calculation of the fitness function. After comparing the optimal position of the selected particles to participate in the next operation, and so on, until the fitness function tends to 0, to get  $R_s$ ,  $L_d$ ,  $L_q$ ,  $\psi_f$  four parameter values, at this time is considered the real value of the system. Then, for the PMSM vector control system, the object fitness function can be defined as Eq. (5).

$$f(R_s, L_d, L_q, \psi_f) = \lambda_1 (i_d - \hat{i}_d)^2 + \lambda_2 (i_q - \hat{i}_q)^2, \quad (5)$$

where  $\lambda_1 = \lambda_2 = 1$ , think that  $i_d$  and  $i_q$  are equally important.

### 3. Basic dung beetle algorithm

The dung beetle algorithm is a new swarm intelligence algorithm, which has four roles: a rolling dung beetle; dung beetles rearing babies; a small dung beetle; the thief dung beetle. This algorithm is mainly inspired by the behaviors of dung beetles such as rolling, dancing, foraging, stealing and reproduction, and has the characteristics of fast convergence, high solution accuracy, and both global exploration and local development [20].

The mathematical model for the dung beetle algorithm is:

#### 1. Solar influence

Dung beetles need the sun to guide them in the rolling process. During the rolling process, the position of dung beetles is updated as follows:

$$\begin{cases} x_i(t+1) = x_i(t) + \alpha \cdot k \cdot x_i(t-1) + b \cdot \Delta x \\ \Delta x = |x_i(t) - X^w| \end{cases}, \quad (6)$$

where:  $t$  denotes the current number of iterations;  $x_i(t)$  denotes the position information of the  $i$ -th dung beetle at the  $t$ -th iteration;  $k \in (0, 0.2)$ ;  $b \in (0, 1)$ ;  $\Delta x$  indicates the degree of variation in light intensity; and  $X^w$  indicates the global worst position;  $\alpha = \pm 1$ .

#### 2. The act of dancing

If the dung beetle encounters an obstacle that prevents it from moving forward, it will need to dance to position itself to obtain a new route, at which point it will use the tangent function  $\tan \theta$  to obtain a new rolling direction with the interval  $[0, \pi]$ , (the dung beetle will not change position when  $\theta = 0$  or  $\theta = \pi/2$ ), at which point the dung beetle's position is updated by the formula:

$$\begin{cases} x_i(t+1) = x_i(t) + \tan \theta |x_i(t) - x_i(t-1)| \\ \theta \in [0, \pi] \end{cases}. \quad (7)$$

#### 3. Dung beetle reproduction

In order to provide a safe environment for dung beetles to lay and breed, a boundary selection strategy is proposed to model the female dung beetle's egg-laying area, defined as:

$$\begin{cases} Lb^* = \max(X^* \times (1 - R), Lb) \\ Ub^* = \min(X^* \times (1 + R), Ub) \end{cases}, \quad (8)$$

where:  $X^*$  denotes the current local optimum position,  $Lb^*$  and  $Ub^*$  denote the lower and upper bounds of the spawning region,  $Lb$  and  $Ub$  denote the lower and upper bounds of the search space, and  $R = 1 - t/T_{\max}$ ,  $T_{\max}$  denote the maximum number of iterations.

For the DBO algorithm, each female produces only one egg per iteration in the region, that is, one solution. As can be seen from Eq. 9, the constraint boundary of the spawning region is dynamically changed, so the spawning position is also dynamic in the iterative process, that is:

$$B_i(t+1) = X^* + b_1 (B_i(t) - Lb^*) + b_2 (B_i(t) - Ub^*), \quad (9)$$

where:  $B_i(t)$  is the position of the  $i$ -th spawning ball at the  $t$ -th iteration,  $b_1$  and  $b_2$  are two independent random vectors of size  $1 \times D$ , and  $D$  denotes the dimensionality of the optimization problem.

When the females have hatched successfully, the young dung beetles will forage and therefore, establish the best foraging areas as:

$$\begin{cases} Lb^b = \max(X^b \times (1 - R), Lb) \\ Ub^b = \min(X^b \times (1 + R), Ub) \end{cases}, \quad (10)$$

where:  $X^b$  is the global optimal position,  $Lb^b$  and  $Ub^b$  are the upper and lower constraint boundaries of the optimal foraging area. The equation for updating the position of a small dung beetle can be defined as:

$$x_i(t+1) = x_i(t) + C_1 (x_i(t) - Lb^b) + C_2 (x_i(t) - Ub^b), \quad (11)$$

where:  $x_i(t)$  denotes the location information of the  $i$ -th small dung beetle at the  $t$ -th iteration,  $C_1$  denotes a random number following a normal distribution, and  $C_2$  denotes a random vector of  $(0, 1)$ .

#### 4. Theft

Since  $X^b$  is the globally optimal location, where it is also the best location for dung beetle stealing behaviour, the location of the stealing dung beetle is updated during the iterative process as:

$$x_i(t+1) = X^b + S \cdot g \left( |x_i(t) - X^*| + |x_i(t) - X^b| \right), \quad (12)$$

where:  $x_i(t)$  denotes the location information of the  $i$ -th stealing dung beetle at the  $t$ -th iteration,  $g$  is a random vector of size  $1 \times D$  that follows a normal distribution, and  $S$  is a constant.

### 4. An improved dung beetle algorithm

The four-position update formula of the original DBO algorithm will cause the populations to cluster together quickly and lose the population diversity at a later stage when the population size is large and the number of iterations is large, thus, increasing the probability of falling into local optimal solutions. To solve this problem, three improvement strategies are proposed in this paper to improve the algorithm's performance. The improved dung beetle algorithm is named the CDBO algorithm, the CDBO can be an interesting algorithm for other applications (such as geometric optimization of machines).

#### 4.1. Population initialization strategy

Chaotic mapping is a method for generating chaotic sequences, which has the characteristics of simple mathematical form, good ergodicity, and strong randomness. In order to solve the problem that the initial particle aggregation will lead to local optimization in the iterative process, this paper proposes a strategy to improve the initial dung beetle population by using Singer chaotic mapping. The expression of Singer chaos mapping is shown in (13).

$$X_{k+1} = \mu \left( 7.86X_k - 23.31X_k^2 + 28.75X_k^3 - 13.302875X_k^4 \right), \quad (13)$$

where  $\mu \in (0.9, 1.08)$  and  $X \in [0, 1]$ . In this paper, we have chosen  $\mu = 1.07$ .

The distribution plots for 5 000 iterations of the Singer chaos mapping are shown in Fig. 2. It can be seen that the Singer chaos mapping distributes the population particles evenly between  $[0, 1]$ . Using this feature can make the search space more homogeneous and increase the dung beetle population diversity and homogeneity, thus, increasing the global search capability.

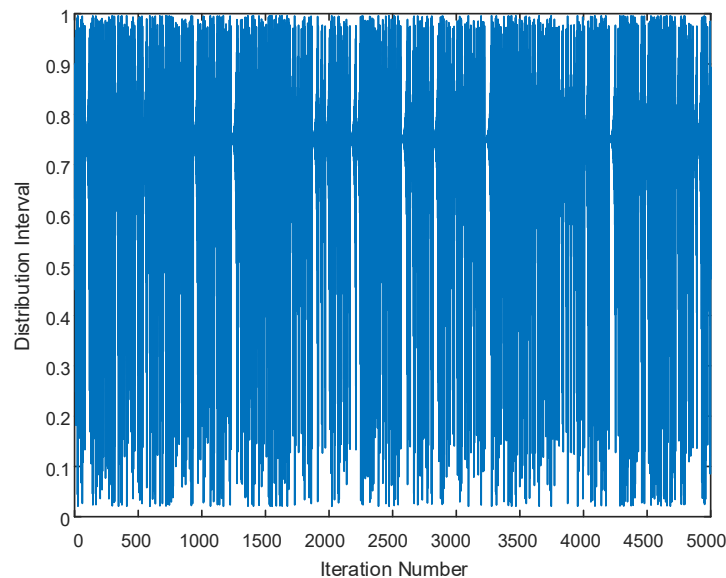


Fig. 2. Singer chaos map of iteration diagram

#### 4.2. Dung beetle reproduction and small dung beetle foraging location update strategy

As seen in dung beetle reproduction Formula (9) and small dung beetle foraging Formula (11), the original DBO algorithm's position update formula later causes the populations to cluster together quickly, losing population diversity and thus, increasing the probability of falling into a local optimum solution. Therefore, based on the original DBO algorithm, a new dung beetle reproduction and small dung beetle foraging location update strategy is designed. This enables both breeding locations and small dung beetles foraging to be searched in space in the form of

a spiral, extending the discoverer's ability to explore unknown regions, helping the algorithm to jump out of the local optimum and effectively improving the algorithm's local search capability.

In this paper, we define the parameter that defines the shape of the logarithmic spiral as  $Z$ , as shown in the following equation:

$$Z = \exp\left(k \cdot \cos\left(\frac{\pi t}{T_{\max}}\right)\right), \quad (14)$$

where:  $k$  is the adjustment factor, and by convention  $k$  is 5;  $t$  is the number of current iterations; and  $T_{\max}$  is the maximum number of iterations.

The mathematical model to achieve the spiral update position is:

$$X(t+1) = D \cdot e^{Zl} \cdot \cos(2\pi l) + X^*(t), \quad (15)$$

where:  $D$  is the object movement distance,  $X$  is the object search position, indicating the current local optimum position, and  $X^*$  is the spiral update position mechanism, as shown in Fig. 3.

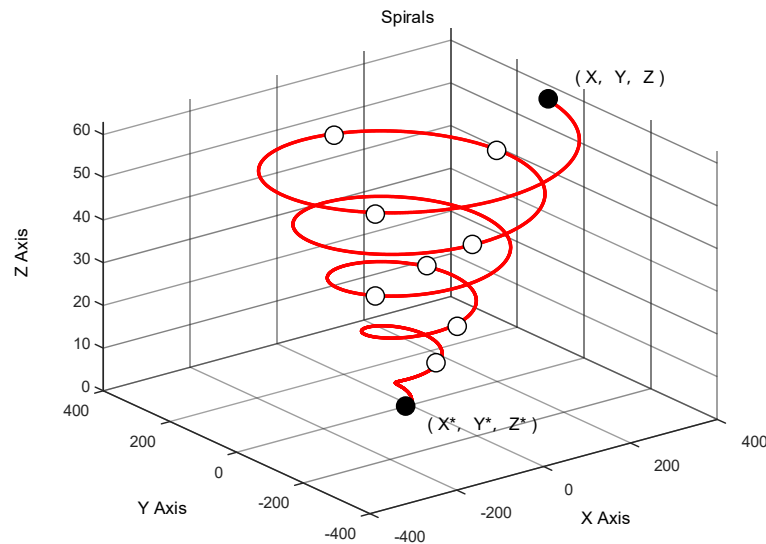


Fig. 3. Map of the spiral update location mechanism

Using the above mathematical model with variable spiral parameters and the updated position of the spiral to improve dung beetle reproduction Eq. (9) and small dung beetle foraging Eq. (11), the improved equations were obtained as:

$$B_i^{t+1} = x_{g_{\text{best}}}^t + e^{Zl} \cdot \cos(2\pi l) \cdot b_1 (B_i^t - Lb^*) + e^{Zl} \cdot \cos(2\pi l) \cdot b_2 (B_i^t - Ub^*), \quad (16)$$

$$x_i^{t+1} = e^{Zl} \cdot \cos(2\pi l) x_i^t + C_1 \cdot (x_i^t - Lb^l) + C_2 \cdot (x_i^t - Ub^l), \quad (17)$$

where  $l = 2 \times \text{rand} - 1$  and  $\text{rand}$  denotes a random number between 0 and 1.

The proposed dung beetle breeding and small dung beetle foraging location update strategy utilizes the cosine parameter for spiral search, which extends the discoverer's ability to explore unknown regions and further improves the local search capability of the algorithm.

### 4.3. Stealing dung beetle location update strategy

Since many algorithms fall into local optima to varying degrees later, affecting algorithm performance, to improve this problem, this paper designs a new strategy for stealing dung beetle position updates. Levy flight is a random wandering strategy conforming to the Levy distribution proposed by the French mathematician Levy, which will randomly generate longer or shorter step sizes while increasing the search range. The Levy flight process that simulates the step size equation is:

$$\text{Levy}(\beta) = \frac{\mu}{|\nu|^{-\beta}}, \quad (18)$$

where  $\text{Levy}(\beta)$  is the Levy distribution with parameter  $\beta$  and  $0 < \beta < 2$ ,  $\mu$  is the distribution with parameter  $N(0, 1)$ .

The position update formula using the Levy flight is:

$$x_i^{t+1} = x_i^t + \alpha L(\beta) (g_{\text{best}}(i) - x_i^t), \quad (19)$$

where:  $x_i^{t+1}$ ,  $x_i^t$  are the positions of the  $(t + 1)$ -nd and  $t$ -rd generations of  $x_i$ , respectively; the scaling factor  $\alpha = 0.01$ ;  $g_{\text{best}}(i)$  is the most available position of the current population; and  $L$  is the Levy step factor obeyed, as shown in the following equation:

$$L \sim \frac{\lambda \Gamma(\beta) \sin\left(\frac{\pi\lambda}{2}\right)}{\pi \cdot s^{1+\beta}}, \quad (20)$$

where  $\beta = 1.5$  and  $\Gamma(\beta)$  is the gamma function.

$$s = \left| \frac{\mu}{\nu^{\frac{1}{\beta}}} \right|, \quad (21)$$

where:  $\mu$  follows the  $N(0, \sigma^2)$  distribution;  $\nu$  follows the  $N(0, 1)$  distribution; and  $\sigma$  is as follows:

$$\sigma = \left\{ \frac{\Gamma(1 + \beta) \sin\left(\frac{\pi\beta}{2}\right)}{\Gamma\left(\frac{1 + \beta}{2}\right) \beta \cdot 2^{\frac{\beta-1}{2}}} \right\}^{\frac{1}{\beta}}. \quad (22)$$

Updating Eq. (12) using the Levy flight strategy above to optimise the location of the stealing dung beetle gives the improved equation as:

$$x_i^{t+1} = \text{Levy} \cdot x_{i_{\text{best}}}^t + S \cdot g \cdot \left( |x_i^t - x_{g_{\text{best}}}^t| + |x_i^t - w \cdot x_{i_{\text{best}}}^t| \right). \quad (23)$$

In this paper, we take  $S = 0.5$ ,  $w$  is to be the adaptive weighting factor, defined as:

$$w = \frac{e^{2 \times (1 - \frac{t}{\max t})} - e^{-2 \times (1 - \frac{t}{\max t})}}{e^{2 \times (1 - \frac{t}{\max t})} + e^{-2 \times (1 - \frac{t}{\max t})}}. \quad (24)$$

The location update strategy for stealing dung beetles designed in this paper enables the stealing dung beetle to perform another Levy flight after each iteration Using the small range search of the Levy flight combined with the long-distance migration property to further expand the search range, effectively avoid falling into local optimum and can improve the convergence accuracy of the algorithm.

## 5. Simulation analysis

### 5.1. Experimental setup

A simulation block diagram of PMSM parameter identification based on the CDBO algorithm was constructed on the MATLAB/SIMULINK software platform as shown in Fig. 4, and the CDBO algorithm was compared with the DBO algorithm, PSO and the GA.

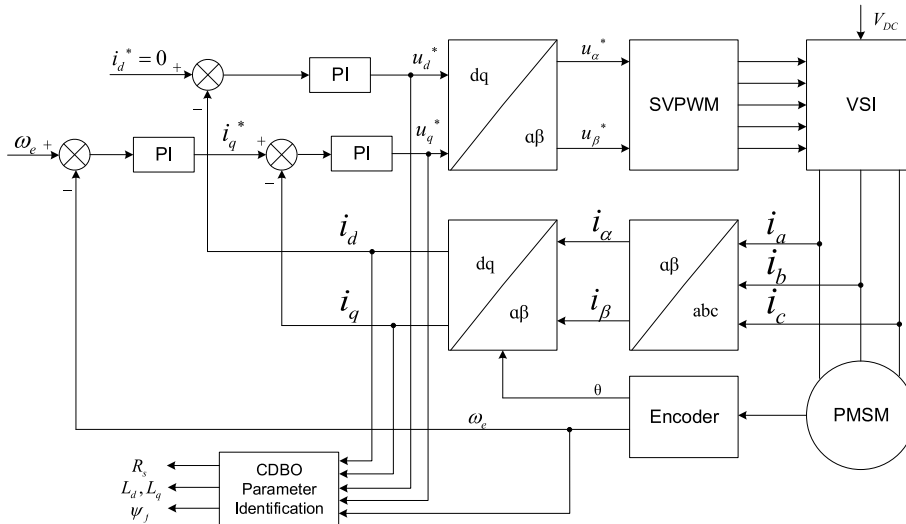


Fig. 4. Simulation block diagram of PMSM parameter identification based on CDBO algorithm

In this simulation experiment the parameters of the PMSM are shown in Table 1. The parameters associated with the initialisation of CDBO and DBO are  $k = 0.1$ ,  $b = 0.3$  and  $S = 0.5$ . The range of the recognition parameters set by the PSO algorithm at the time of recognition is:  $R_s \in (0, 2)$ ,  $L_d \in (0, 0.1)$ ,  $L_q \in (0, 0.1)$ ,  $\psi_f \in (0, 0.2)$ . The PSO algorithm has an initial

Table 1. PMSM parameters

Parameters	Parameter values
Polar logarithm	4
Stator resistance $R_s/\Omega$	1
$d$ -axis inductors $L_d/\text{mH}$	0.8
$q$ -axis inductors $L_q/\text{mH}$	0.8
Main magnetic pole flux $\psi_f/\text{Wb}$	0.1827
Rotational inertia $J/\text{kg}\cdot\text{m}^2$	0.003
Rated speed $\omega_e/(\text{r}/\text{min})$	2000

correlation parameter of  $C_1 = C_2 = 2$  and an inertia weight of  $\omega = 0.5$ . The crossover probability of the GA is 0.68, the probability of variation is 0.0005. All algorithms have a number of iterations of 100 and a population size of 50, all run independently 30 times.

### 5.2. Experimental results and analysis

Because the intelligent algorithm is different from the traditional optimization method, the test function is needed to verify the performance of the optimization algorithm. We used four test functions in IEEE CEC-2017 for algorithm performance verification where  $f_1 - f_2$  is a high-dimensional unimodal function and  $f_3 - f_4$  is a high-dimensional multi-modal function. The improved CDBO algorithm is compared with the standard particle swarm optimization algorithm (PSO) to find the best performance. The specific information of the selected international general test function is shown in Table 2. After testing, the error and iteration curves of different algorithms for different test functions are shown in Fig. 5.

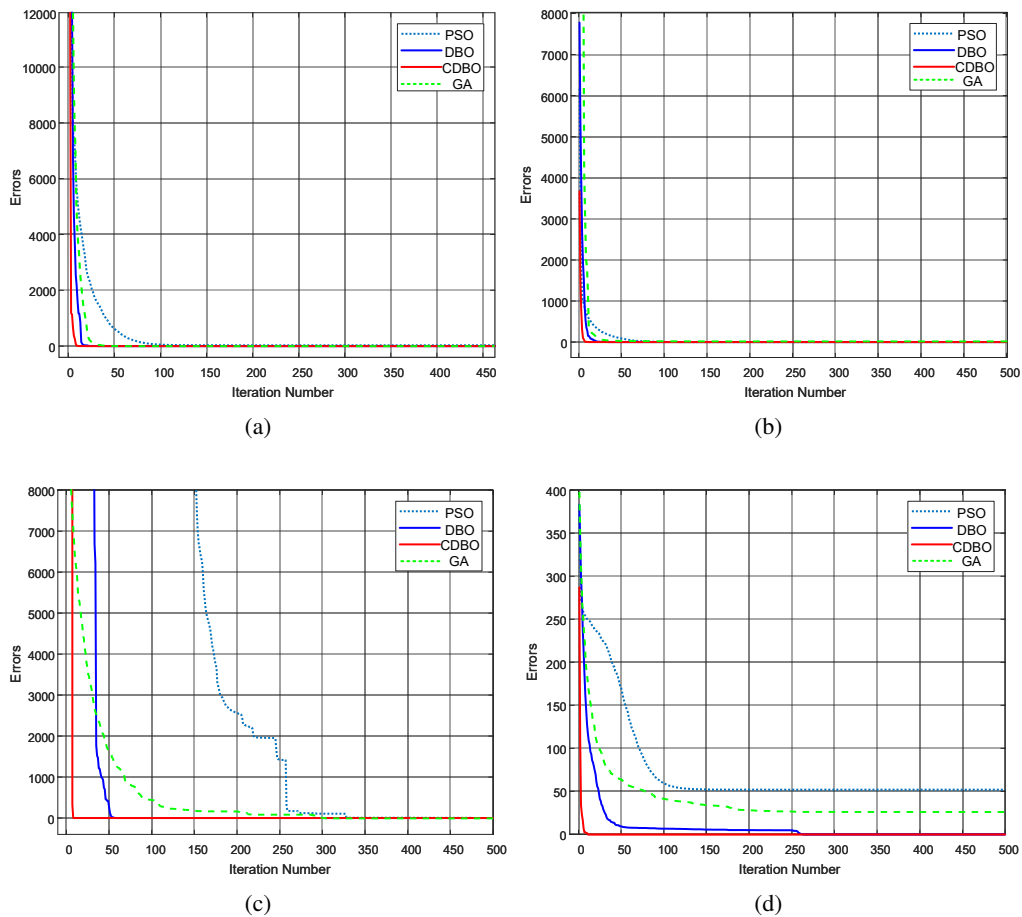


Fig. 5. Testing the effect of the  $f_1 \sim f_4$  search

Table 2. International examples of extreme value optimization of continuous functions

Functions	Dimensionality	Range of values	Optimal solution value
$f_1 = \sum_{i=1}^n x_i^2$	30	[-100, 100]	0
$f_2 = \sum_{i=1}^n \left( \sum_{j=1}^n x_j \right)^2$	30	[-100, 100]	0
$f_3 = \sum_{i=1}^n (x_i + 0.5)^2$	30	[-100, 100]	0
$f_4 = \sum_{i=1}^n \left[ x_i^2 - 10 \cos(2\pi x_i) + 10 \right]$	30	[-5.12, 5.12]	0

It can be seen from Fig. 5 that the CDBO algorithm is not only superior to DBO, PSO and GA algorithms in fitness convergence, but also that CDBO algorithm is significantly less than DBO, PSO and GA algorithms in the number of iterations. At about the 10-th iteration, the error of the test function has converged to 0, and the convergence speed is fast. As can be seen in Fig. 5(c), the convergence speed of PSO and GA algorithms is slow and the stability is poor, but the CDBO algorithm proposed in this paper can still converge to 0 around the 10th generation without fluctuation. As can be seen in Fig. 5(d) the DBO algorithm begins to converge when iterating about 40 generations, converges to 0 until 260 generations, and then becomes stable. PSO and GA algorithms converge to stable after 50 in about 100 generations, and the error is large. However, the proposed CDBO algorithm can still converge to 0 around the 10th generation with almost no fluctuation.

In summary, compared with DBO, PSO and the GA, the proposed CDBO algorithm has faster convergence speed and better stability.

The iterative identification processes of the three algorithms are shown in Figs. 6–8 for a rotational speed of  $\omega = 1500$  r/min and a load torque of 10 N·m.

From Fig. 6, it can be seen that the CDBO algorithm proposed in this paper converges steadily around the true value at about 6 iterations, and there is almost no fluctuation after convergence. The DBO algorithm converges around the true value at about 8 iterations, but fluctuates at 15–20 iterations, and the error is small. the PSO algorithm converges around the true value at about 62 iterations, but fluctuates more after convergence, resulting in a large error. The GA converges to the true value in about 15 iterations, but it will fluctuate several times and cause errors after convergence. From Fig. 7, it can be seen that all four algorithms converge to near the true value at smaller iterations, but the PSO algorithm has significant fluctuations at iteration 15–20, resulting in larger errors. From Fig. 8, it can be seen that the CDBO algorithm proposed in this paper converges to near the true value after about 6 iterations, and there is almost no fluctuation after convergence. The DBO algorithm converges to the true value after about 15 iterations, and then

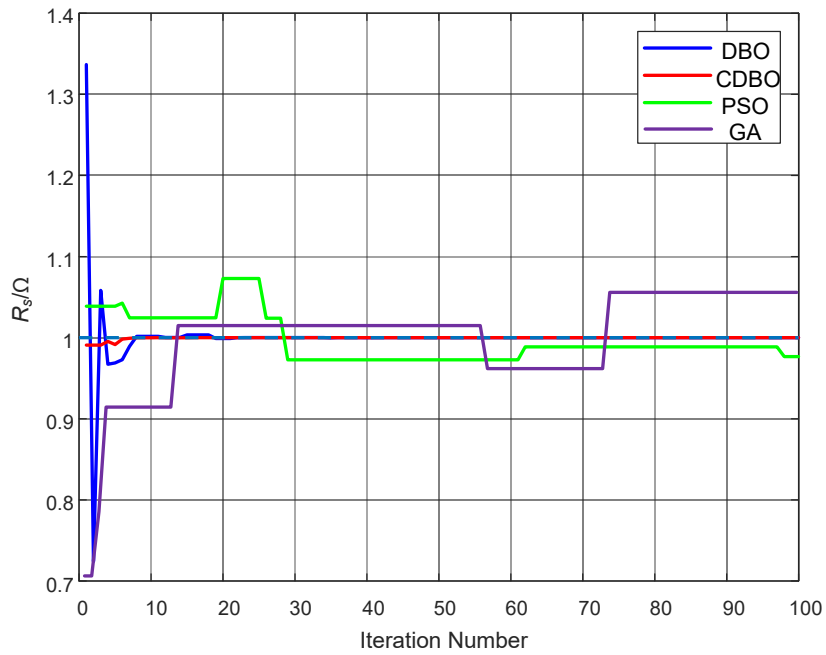


Fig. 6. Evolutionary process of  $R_s$  identification

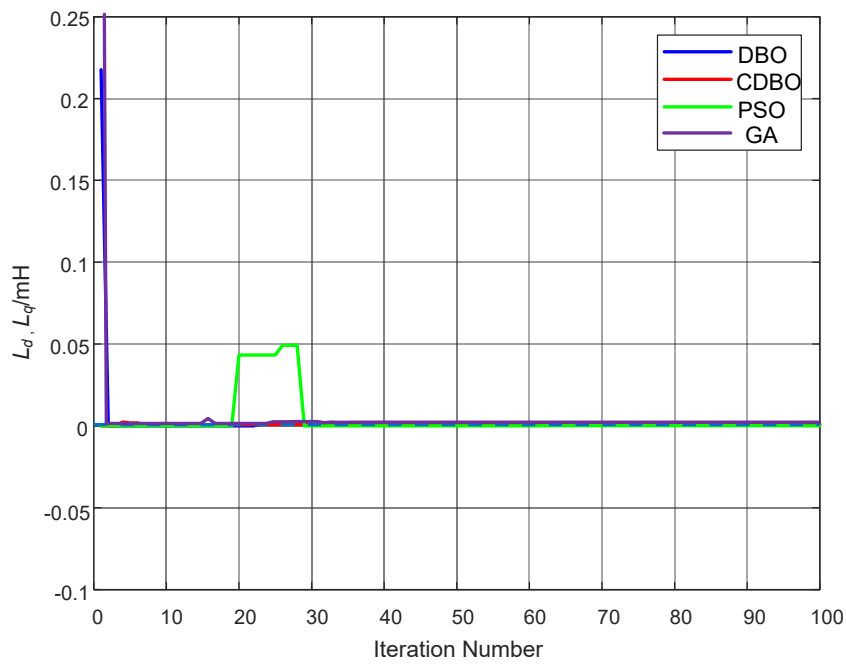


Fig. 7. Evolutionary process of  $L_d, L_q$  identification

the fluctuation is small. The GA converges after about 20 iterations, but PSO algorithm converges slowly and has a large error.

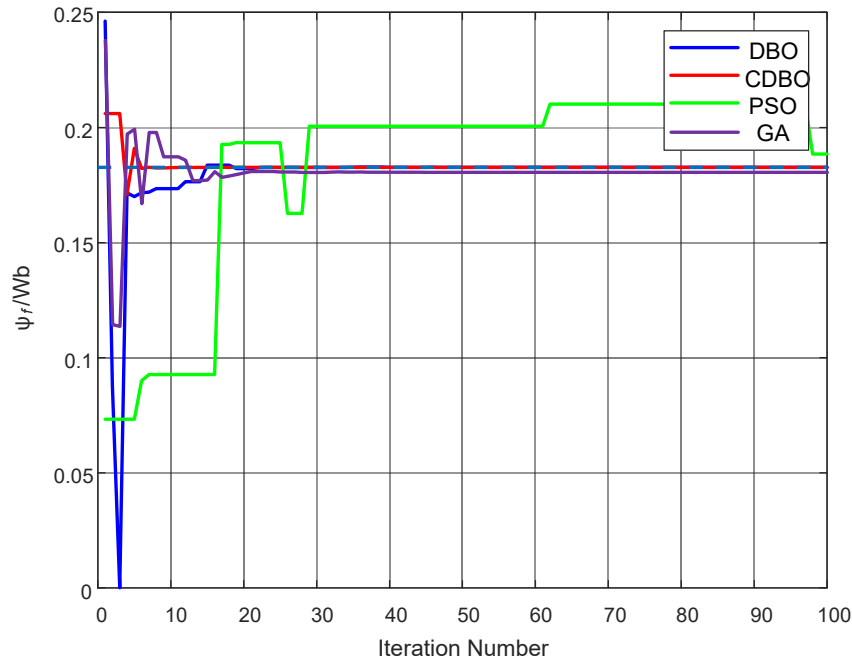


Fig. 8. Evolutionary process of  $\psi_f$  identification

As shown above, the CDBO algorithm proposed in this paper is effective and feasible to be applied to the parameter identification of the PMSM system, and has the advantages of fast convergence, high stability and high accuracy compared with DBO, PSO and the GA.

The results of the simulation waveforms constructed by MATLAB/SIMULINK based on the CDBO algorithm to identify the PMSM parameters are shown in Figs. 9 to 11. And as shown in Fig. 9, in the process of identifying the stator resistance, it converges to near the true value in about 0.04 seconds, and the error fluctuation is small.

As shown in Fig. 9, in the process of identifying the  $d - q$  axis inductance, it converges to the true value in about 0.1 seconds, and the error fluctuation is small. As shown in Fig. 11, the process of identifying the magnetic chain converges to the true value in about 0.025 seconds with small error fluctuations.

As can be seen from Table 3, compared with the DBO, PSO and GA algorithms, the proposed CDBO algorithm is significantly better than the other three methods in multi-parameter identification, and the results can all converge to near the true value with less error.

It can be seen that the CDBO algorithm proposed in this paper is not only effective and feasible in identifying parameters, but also has the characteristics of high accuracy, few convergence generations, fast speed and stability.

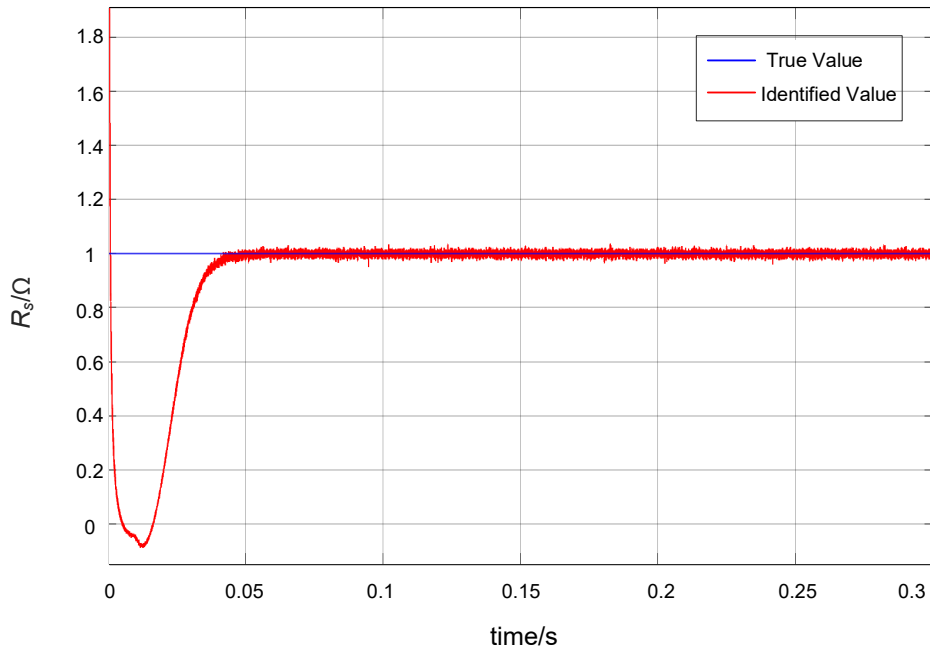


Fig. 9. CDBO-based  $R_s$  identification process

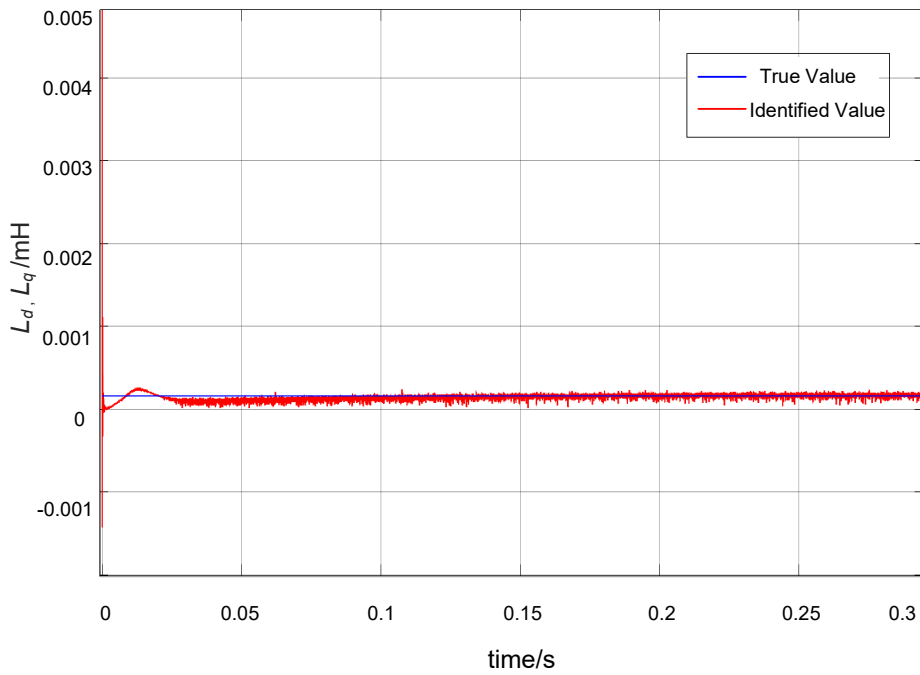


Fig. 10. CDBO-based  $L_d, L_q$  identification process

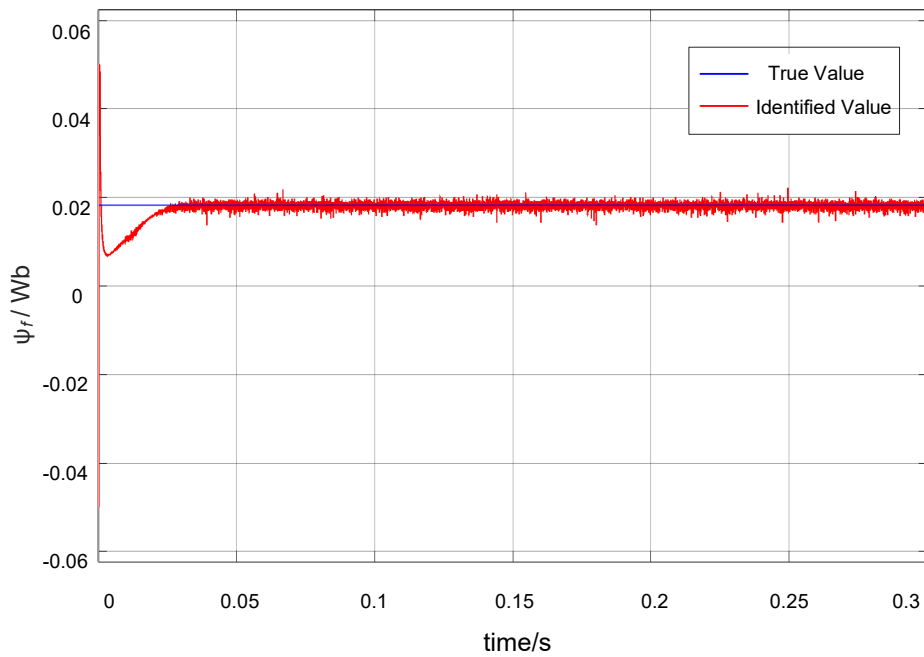


Fig. 11. CDBO-based  $\psi_f$  identification process

Table 3. Comparison of three parameter identification algorithms for PMSM

Parameters to be identified	Actual value	Identifying value				Error (%)			
		DBO	CDBO	PSO	GA	DBO	CDBO	PSO	GA
$R_s/\Omega$	1	0.9985	0.9995	0.97767	0.9892	0.15	0.05	2.33	1.1
$L_d/mH$	0.8	0.7998	0.7999	0.6947	0.7325	0.025	0.0125	13.16	8.4
$L_{qg}/mH$	0.8	0.7998	0.7999	0.6947	0.7325	0.025	0.0125	13.16	8.4
$\psi_f/Wb$	0.1827	0.1823	0.1826	0.1885	0.1853	0.2189	0.05	3.17	1.4

## 6. Conclusion

In this paper, a new creative dung beetle optimization (CDBO) algorithm is proposed for the parameter identification problem of a permanent magnet synchronous motor (PMSM) and implemented under the vector control method of  $i_d = 0$ . First, the proposed Singer chaotic mapping improves the strategy for initializing dung beetle populations, which can uniformly initialize population states, increase population diversity and improve global search performance; second, the location update strategy designed in this paper increases the spatial search range of the algorithm, improves the local search performance, and moreover improves the convergence

accuracy of the algorithm. In addition, four commonly used international test functions are used to compare the performance of PSO, DBO and GA algorithms. The test function results show that the performance of the CDBO algorithm is better than PSO, DBO and GA algorithms, and it has the characteristics of less convergence algebra, high identification accuracy and strong stability, and through the parameter identification simulation results show that the algorithm can quickly and accurately identify the PMSM resistance, inductance and magnetic chain parameters, and so on. It proves the effectiveness of the CDBO algorithm in the field of PMSM parameter identification and also provides a new solution to the PMSM parameter identification problem.

### Acknowledgements

This work was supported by the National Natural Science Foundation of China (Grant No. 61803345); Science and Technology Development Project of Henan Province (212102210024, 222102220064, 222102240005).

### References

- [1] Krzysztofiak M., Zawilak T., Tarchala G., *Online control signal-based diagnosis of interturn short circuits of PMSM drive*, Archives of Electrical Engineering, vol. 72, no. 1, pp. 67–69 (2023), DOI: [10.1515/ae-2015-0007](https://doi.org/10.1515/ae-2015-0007).
- [2] An Q., Li S., *On-line parameter identification for vector controlled PMSM drives using adaptive algorithm*, Vehicle Power & Propulsion Conference, Harbin, China, pp. 1–6 (2008).
- [3] Underwood S.J., Husain I., *Online Parameter Estimation and Adaptive Control of Permanent-Magnet Synchronous Machines*, IEEE Transactions on Industrial Electronics, vol. 57, no. 7, pp. 2435–2443 (2010), DOI: [10.1109/TIE.2009.2036029](https://doi.org/10.1109/TIE.2009.2036029).
- [4] Fan S., Luo W., Zou J., *A hybrid speed sensorless control strategy for PMSM Based on MRAS and Fuzzy Control*, Power Electronics & Motion Control Conference, Harbin, China, pp. 2976–2980 (2012).
- [5] Wang S., Liu M., Shi S., Yang G., *Identification of PMSM based on EKF and Elman neural network*, 2009 IEEE International Conference on Automation and Logistics, Shenyang, China, pp. 1459–1463 (2009).
- [6] Jing C., Yan Y., Lin S., *A Novel Moment of Inertia Identification Strategy for Permanent Magnet Motor System Based on Integral Chain Differentiator and Kalman Filter*, Energies, vol. 14, no. 2, pp. 235–246 (2020), DOI: [10.3390/en14010166](https://doi.org/10.3390/en14010166).
- [7] Liu Y., Zhao J., Wang Q., *An off-line parameter identification method for indirect vector controlled induction motor drive*, Transactions on Power Systems, vol. 23, no. 7, pp. 21–26 (2008), DOI: [10.3321/j.issn:1000-6753.2008.07.004](https://doi.org/10.3321/j.issn:1000-6753.2008.07.004).
- [8] Li K., Liu L., Zhai J., *The improved grey model based on particle swarm optimization algorithm for time series prediction*, Engineering Applications of Artificial Intelligence, vol. 55, no. 3, pp. 285–291 (2016), DOI: [10.1016/j.engappai.2016.07.005](https://doi.org/10.1016/j.engappai.2016.07.005).
- [9] Fu X., Gu H., Chen G., *Permanent Magnet Synchronous Motors Parameters Identification Based on Cauchy Mutation Particle Swarm Optimization*, Transactions of China Electrotechnical Society, vol. 29, no. 5, pp. 127–131 (2014), DOI: [10.3969/j.issn.1000-6753.2014.05.016](https://doi.org/10.3969/j.issn.1000-6753.2014.05.016).
- [10] Cao Y., Mao R., Feng L., *Multi-parameter identification of permanent magnet synchronous motor based on improved sparrow search algorithm*, Advanced Technology of Electrical Engineering and Energy, vol. 41, no. 5, pp. 26–34 (2022), DOI: [10.3969/j.issn.1000-1158.2017.05.24](https://doi.org/10.3969/j.issn.1000-1158.2017.05.24).

- [11] Zhang L., Zhang P., Liu Y., *Parameter Identification of Permanent Magnet Synchronous Motor Based on Variable Step-Size Adaline Neural Network*, Transactions on Power Systems, vol. 33, no. S2, pp. 377–384 (2018), DOI: [10.19595/j.cnki.1000-6753.tces.L80266](https://doi.org/10.19595/j.cnki.1000-6753.tces.L80266).
- [12] Rahimi A., Bavafa F., Aghababaei S., *The online parameter identification of chaotic behaviour in permanent magnet synchronous motor by Self-Adaptive Learning Bat-inspired algorithm*, International Journal of Electrical Power & Energy Systems, vol. 78, pp. 285–291 (2016), DOI: [10.1016/j.ijepes.2015.11.084](https://doi.org/10.1016/j.ijepes.2015.11.084).
- [13] Li P., Ding Q., *OSTU segmentation algorithm based on sparrow algorithm optimization*, Electronic Measurement Technology, vol. 44, no. 19, pp. 148–154 (2021), DOI: [10.19651/j.cnki.emt.2107707](https://doi.org/10.19651/j.cnki.emt.2107707).
- [14] Lin Z., Liu Y., *Dispersed chaotic swarm oscillation algorithm merged with spiral strategy*, Application Research of Computers, vol. 38, no. 10, pp. 3060–3071 (2021), DOI: [10.19734/j.issn.1001-3695.2021.03.0086](https://doi.org/10.19734/j.issn.1001-3695.2021.03.0086).
- [15] Wu Z., Song F., *Whale optimization algorithm based on improved spiral update position model*, Systems Engineering – Theory & Practice, vol. 39, no. 11, pp. 2928–3944 (2019), DOI: [10.12011/1000-6788-2018-2156-17](https://doi.org/10.12011/1000-6788-2018-2156-17).
- [16] Ji P., Chen F., Xu T., Huo Y., Qi Q., *Qpso-svm algorithm optimized based on Levy flight strategy fusion and adaptive variation factor*, Journal of Yunnan Minzu University, vol. 1, no. 8 (2023), DOI: [53.1192.N.20230310.1023.006](https://doi.org/53.1192.N.20230310.1023.006).
- [17] Cui M., Jin Q., *Grey Wolf Optimization Algorithm Based on Levy Flight Strategy*, Computer & Digital Engineering, vol. 50, no. 5, pp. 948–958 (2022), DOI: [10.3969/j.issn.1672-9722.2022.05.006](https://doi.org/10.3969/j.issn.1672-9722.2022.05.006).
- [18] Aydodu I., Akn A., Saka M.P., *Design optimization of real world steel space frames using artificial bee colony algorithm with Levy flight distribution*, Advances in Engineering Software, vol. 92, pp. 1–14 (2016), DOI: [10.1016/j.advengsoft.2015.10.013](https://doi.org/10.1016/j.advengsoft.2015.10.013).
- [19] Kamaruzaman A.F., Zain A.M., Yusuf S.M., *Levy Flight Algorithm for Optimization Problems – A Literature Review*, Applied Mechanics & Materials, vol. 421, pp. 496–501 (2013), DOI: [10.4028/www.scientific.net/AMM.421.496](https://doi.org/10.4028/www.scientific.net/AMM.421.496).
- [20] Xue J., Shen B., *Dung beetle optimizer: a new meta-heuristic algorithm for global optimization*, The Journal of Supercomputing, vol. 79, no. 7, pp. 7305–7336 (2022), DOI: [10.1007/s11227-022-04959-6](https://doi.org/10.1007/s11227-022-04959-6).